MVPatch: More Vivid Patch for Adversarial Camouflaged Attacks on Object Detectors in the Physical World

Zheng Zhou, *Graduate Student Member, IEEE,* Hongbo Zhao, *Senior Member, IEEE,*
Ju Liu, *Senior Member, IEEE,* Qiaosheng Zhang, Liwei Geng,
Shuchang Lyu, *Graduate Student Member, IEEE,* and Wenquan Feng

Abstract—Recent investigations demonstrate that adversarial patches can be utilized to manipulate the result of object detection models. However, the conspicuous patterns on these patches may draw more attention and raise suspicions among humans. Moreover, existing works have primarily focused on enhancing the efficacy of attacks in the physical domain, rather than seeking to optimize their stealth attributes and transferability potential. To address these issues, we introduce a dual-perception-based attack framework that generates an adversarial patch known as the More Vivid Patch (MVPatch). The framework consists of a model-perception degradation method and a human-perception improvement method. To derive the MVPatch, we formulate an iterative process that simultaneously constrains the efficacy of multiple object detectors and refines the visual correlation between the generated adversarial patch and a realistic image. Our method employs a model-perception-based approach that reduces the object confidence scores of several object detectors to boost the transferability of adversarial patches. Further, within the human-perception-based framework, we put forward a lightweight technique for visual similarity measurement that facilitates the development of inconspicuous and natural adversarial patches and eliminates the reliance on additional generative models. Additionally, we introduce the naturalness score and transferability score as metrics for an unbiased assessment of various adversarial patches' natural appearance and transferability capacity. Extensive experiments demonstrate that the proposed MVPatch algorithm achieves superior attack transferability compared to similar algorithms in both digital and physical domains while also exhibiting a more natural appearance. These findings emphasize the remarkable stealthiness and transferability of the proposed MVPatch attack algorithm.

Index Terms—Adversarial example, patch attack, physical attack, neural network, transferable and stealthy attack

I. INTRODUCTION

DEEP Neural Networks (DNNs) have achieved remarkable performance in manifold fields, such as computer vision

Zheng Zhou, Hongbo Zhao, Liwei Geng, Shuchang Lyu and Wenquan Feng are with the School of Electronic and Information Engineering, Beihang University, Beijing, 100191, China and Wenquan Feng is also with Hefei Inovation Research Institute of Beihang University, Beihang University, Hefei, 230071, China (e-mail: zhengzhou@buaa.edu.cn; bhzhb@buaa.edu.cn; liviageng@buaa.edu.cn; lyushuchang@buaa.edu.cn; buaafwq@buaa.edu.cn).

Ju Liu is with the School of Information Science and Engineering, Shandong University, Qingdao, 266237, China (e-mail: juliu@sdu.edu.cn).

Qiaosheng Zhang is with Shanghai Artificial Intelligence Laboratory, Shanghai, 200032, China (e-mail: zhangqiaosheng@pjlab.org.cn).
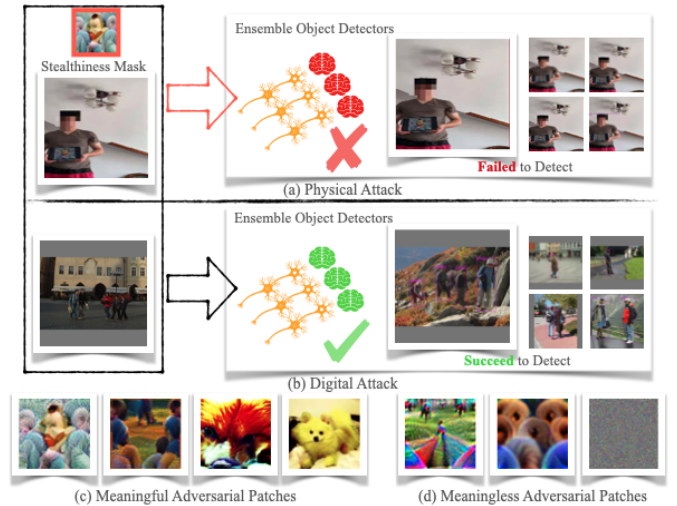
Fig. 1. Introduction to the attack scenarios of MVPatch and illustration of the meaningful and meaningless adversarial patches. (a) demonstrates that MVPatch can make a person invisible to detectors in the real world, while (b) demonstrates that detectors can successfully distinguish a person in the digital world. (c) and (d) demonstrate both diverse meaningful adversarial patches [1] and meaningless adversarial patches [2], [3], respectively.

[4]–[7], natural language processing [8], [9], and automatic speech recognition [10], [11]. However, due to their lack of interpretability, DNNs are vulnerable to Adversarial Examples (AEs) [12]–[14], which raises concerns about their reliability in security-critical applications such as face recognition [15], [16] and autonomous driving [17], [18]. In general, AE attacks can be categorized into two types: Digital Attack (DA) [12], [13], [19]–[26], which involves introducing digital perturbations into the input image to carry out the attack, and Physical Attack (PA) [1]–[3], [16], [27]–[38], which directly targets real-world objects using adversarial perturbations, as illustrated in Fig.1(b) and Fig.1(a), respectively.

Object Detection Models (ODMs) [39]–[41], comprised of deep neural layers, are extensively utilized in real-world applications such as people tracking [42], pedestrian and vehicle re-identification (Re-ID) [43], [44], and remote sensing [45]. Although ODMs enhance human convenience and improve the quality of life, they simultaneously pose a considerable risk to individual privacy and sensitive personal information [1]–[3], [32]. Furthermore, the capability of physical attacks to be transferred amplifies the vulnerability of ODMs [46]–[48]. In

real-world scenarios, AEs could be often observed which are quasi-imperceptible to humans. For example, as depicted in Fig.1, an intruder appears under a surveillance camera holding an adversarial patch, which is camouflaged as Van Gogh's painting, and the DNN-based object detection system will fail. It can even be said that the intruder is invisible under the camera, which will seriously threaten the public safety system Hence, it is imperative to conduct a thorough investigation into PA on ODMs.

Adversarial Patches (APs) [30] have emerged as a potent means to manipulate ODMs within the physical realm, offering several advantages such as input-independence and scene-independence, with substantial real-world impacts [3], [15], [22], [33], [49], [50]. However, much of the extant literature emphasizes enhancing the efficacy of the attack within this physical sphere, rather than seeking to optimize its stealth attributes and transferability potential. Hu et al. [1] considered how to improve the stealthiness of the adversarial patch by Generative Adversarial Network (GAN) [51]. In contrast, Guesmi et al. [38] proposed a lightweight approach to generate natural patches without GAN. Moreover, many scholars have endeavored to augment APs' transferability. A case in point is the research by Wang et al. [46], who honed AP transferability within automated checkout systems through a bias-guided arrangement. In a similar endeavor, Wei et al. [47] devised a Pay No Attention (PNA) attack, wherein attention gradients are disregarded during backpropagation, thereby effectively improving backpropagation's linearity. Furthermore, Huang et al. [48] modified a single surrogate model into a diverse ensemble structure, yielding more transferable adversarial examples. Nevertheless, numerous challenges persist, which include the substantial computational resource requirements associated with the use of GAN during the training process, and an unrelenting research focus on enhancing the stealthiness [1]–[3], [28], [29], [31], [32], [35], [38], [52], [53] and transferability [46]–[48] of APs. Significantly, there remains limited research simultaneously addressing both stealthiness and transferability issues related to APs, with an additional focus on computational resource efficiency.

To bridge this gap, we propose a dual-perception-based framework to generate a potent adversarial patch, referred to as the MVPatch (More Vivid Patch). This attack framework offers remarkable stealthiness and transferability capacities for attacking against ODMs. To improve the transferability potential, we present a model-perception degradation method for ensemble multiple object detectors achieved through the ensemble attack loss function. Additionally, to enhance the stealthiness attributes, we present a human-perception improvement method realized by the Compared Specified Image Similarity (CSS) loss function, which allows for the generation of natural and stealthy adversarial patches without the reliance on additional generative models. By integrating both the model-perception-based method and the human-perception-based method, we can generate a more powerful adversarial patch with significant transferable attack ability and invisibility. Moreover, we introduce the naturalness score and the transferability score as experimental evaluation metrics to assess the attack performance regarding stealthiness and

transferability. We exploit the YOLOv2, YOLOv3, YOLOv3-tiny, YOLOv4, and YOLOv4-tiny as threat models and Faster RCNN, SSD, and YOLOv5 as transfer attack models. Based on extensive experiments conducted in both digital and physical scenarios, along with several independent subjective surveys, our proposed MVPatch consistently generates more natural and transferable results compared to several state-of-the-art baselines. We present the primary specialization of MVPatch, along with the distinguishing features of adversarial patches that possess meaning and those that are devoid of meaning. The main contributions of this work can be summarized as follows:

- To the best of our knowledge, we are the first to propose a dual-perception-based attack framework for generating an adversarial patch (MVPatch). This patch offers both stealthiness and transferability by exploiting both model-perception-based and human-perception-based methods.
- We present the model-perception-based method, an attack method that reduces the object confidence scores of an ensemble of multiple object detectors using an ensemble attack loss function. This enhances the transferability of the adversarial patches, significantly improving attack performance in both digital and physical domains compared to state-of-the-art baselines.
- We propose a human-perception-based method, a lightweight visual similarity measurement method that generates natural and stealthy adversarial patches without the need for additional generative models. This allows us to generate patches based on specific images.
- We employ naturalness and transferability scores as evaluation metrics to assess the naturalness and attack transferability of the diverse adversarial patches in our experiment.
- We perform a comprehensive analysis of the transfer attack performance and naturalness of the proposed method, using both meaningful and meaningless patch approaches in a variety of digital and physical scenarios.

The remainder of this paper is organized as follows. Section II provides a concise literature review on adversarial examples and adversarial patches in various scenarios, encompassing both digital and physical contexts. In Section III, we introduce the definition and characteristics of adversarial patch attacks, along with detailed information regarding the input and output of the threat models. The generation process of our proposed MVPatch is then presented in this section. Section IV introduces the environment and dataset in the experiment, followed by the provision of relevant experimental details. Additionally, we propose evaluation metrics for the experiment. Section V presents empirical evidence that showcases the effectiveness of the proposed MVPatch through comprehensive evaluations conducted in both digital and physical environments. Ultimately, we summarize the paper and present the further research directions in Section VI.

II. RELATED WORK

In this section, we briefly review the literature related to adversarial examples and adversarial patches in diverse

scenarios, such as in the digital domains and physical domains. Furthermore, we discuss the recent issues to be solved and present the necessity of our work.

A. Digital Attack

Adversarial Examples (AEs) are elaborately designed perturbations that are imperceptible to humans but could mislead Deep Neural Networks (DNNs). In 2014, Szegedy et al. [12] discovered a special property of DNNs known as Adversarial Examples (AEs). They successfully attacked a DNN using the L-BFGS algorithm, causing it to produce incorrect predictions. In 2015, Goodfellow et al. [13] introduced the Fast Gradient Sign Method (FGSM), which improved the effectiveness and success rates of attacks on neural network classification models. Kurakin et al. [22] developed the Basic Iterative Method (BIM) and demonstrated the application of AEs in the physical world. Papernot et al. [23] focused on partial attack and presented the Jocobian-Based Saliency Map Attack (JSMA) algorithm. Madry et al. [19] proposed Project Gradient Descent (PGD), an innovative framework that combines attack and defense algorithms to enhance the robustness of DNNs. There are numerous varieties of adversarial attacks in the digital domain, e.g., Deepfool [21], C&W [20], ZOO [24], Universal Perturbation [25], One-Pixel attack [26] and some attacks on large language vision models [54]–[56].

B. Physical Attack

Recently, it has been observed that printed AEs can effectively deceive neural network models in the physical domain. Athalya et al. [27] developed robust three-dimensional AEs that can mitigate the impact of diverse angle transformations. Sharif et al. [28] successfully attacked facial recognition systems by constructing adversarial eyeglasses, while Komkov et al. [29] proposed the construction of an adversarial hat for the same purpose. In 2018, Brown et al. [30] introduced the concept of Adversarial Patch (AP). Liu et al. [31] proposed DPatch to deceive object detection models, while at around the same time, Thy et al. [2] introduced AdvPatch to mislead automated surveillance systems. Wu et al. [32] presented the AdvCloack to make humans invisible in the object detector. Hu et al. [1] designed a more natural patch based on the AdvPatch [2]. Xu et al. [33] proposed to construct an adversarial T-shirt to mislead the object detection systems. Huang et al. [34] introduced the Transfer-based Self-ensemble Attack (T-SEA) for attacking object detectors using ensemble attacks, effectively improving the transferable attack performance. Hu et al. [3] proposed the Toroidal-Cropping-based Expandable Generative Attack (TC-EGA) algorithm, which applies adversarial textures to clothing to improve the stealthiness of the adversarial patch. Wang et al. [35] constructed the adversarial patch based on the attention mechanism for the car camouflage. Wei et al. [16] investigated methods to enhance the attack performance of adversarial patches by focusing on their spatial positioning. Liu et al. [36] proposed a Perceptual-Sensitive Generative Adversarial Network (PS-GAN) to enhance the visual fidelity and attacking performance for the adversarial patches. Xue et al. [37] presented the Diffusion-Based Projected Gradient Desent

(DIff-PGD) to generate realistic adversarial examples by using diffusion models. Guesmi et al. [38] proposed AdvART to attack object detectors by a simple method without generative models.

Despite the significant results achieved by prior research on adversarial patches in the physical world, there are still some issues to be addressed, such as the trade-off between transferability [1], [34], [57] and stealthiniess [3], [27], [29], [32], [33], [35]–[38], [58] of the adversarial patch. Furthermore, most recent research focuses on generating meaningless adversarial patches. The meaningless adversarial patch means that has no sense for human eye perception as Fig.1(d) illustrates. To the best of our knowledge, only one study has systematically examined the investigation of meaningful and transferable adversarial patches through the utilization of a generative adversarial network (GAN) by Hu et al. [1]. However, training a generative adversarial network is challenging and computationally expensive. To address these issues, we propose the MVPatch algorithm, which outperforms other state-of-the-art baseline methods in terms of transferable and stealthy attacks both in the digital and physical scenarios while maintaining a lightweight approach.

III. METHODOLOGY

In this section, we first introduce the definition and characteristics of adversarial patch attacks and then detail the input and output information of threat models. Finally, we summarize the entire generation process of MVPatch in this section.

A. Problem Formulation

The objective of this study is to generate a malicious image $\mathcal{I}^*$ with an adversarial patch from a benign image $\mathcal{I}$, to deceive object detection models. The complete process of generating the adversarial patch is illustrated in Fig.2. Typically, the malicious images with adversarial patches can be formulated as:

$$\mathcal{I}^* = (1 - \mathcal{M}) \odot \mathcal{I} + \mathcal{M} \odot \mathcal{P}, \qquad (1)$$

where $\mathcal{M}$ represents the patch mask, which determines the size, shape, and location of the adversarial patch $\mathcal{P}$. The $\odot$ symbol denotes the Hadamard product, which multiplies the elements of the corresponding positions in the matrices $\mathcal{M}$, $\mathcal{I}$, and $\mathcal{P}$. We denote the object detection model as $f(x) : x \in \mathbb{R}^{\mathbf{H} \times \mathbf{W} \times \mathbf{C}} \mapsto \mathcal{Y} \in \mathbb{R}^6$. x is input image and $\mathcal{Y}$ is label of object. The generation of adversarial patches can be viewed as a constrained optimization problem:

$$f(\mathcal{I}^*) \neq f(\mathcal{I}) \quad \text{s.t.} \, \|\mathcal{I}^* - \mathcal{I}\| \longrightarrow \mathcal{P}, \qquad (2)$$

where $\mathcal{P}$ represents the adversarial patch generated under the constraints of $\|\mathcal{I}^* - \mathcal{I}\| \longrightarrow \mathcal{P}$, while satisfying $f(\mathcal{I}^*) \neq f(\mathcal{I})$. Finding a closed-form solution for this optimization problem is not feasible due to the non-convex nature of the deep neural network model $f(\cdot)$. Therefore, to approximately solve this optimization problem, we utilize the following equation:

$$\underset{\mathcal{P}}{\operatorname{argmax}} \, \mathcal{L}(f(\mathcal{I}^*), f(\mathcal{I})), \qquad (3)$$
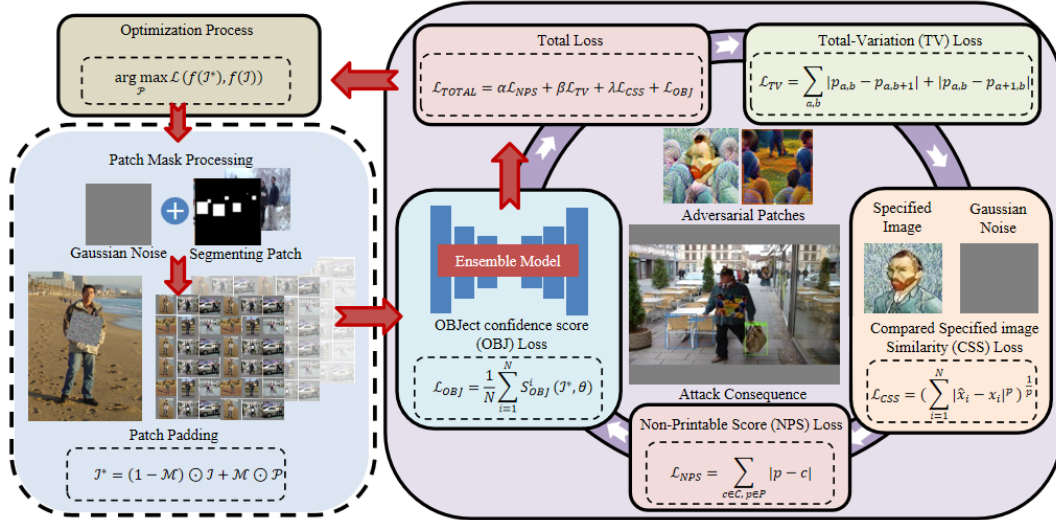
Fig. 2. The MVPatch pipeline involves embedding masks into benign images and applying them to object detectors to determine the object confidence scores. To achieve improved attack performance, the algorithm minimizes various losses, such as TV loss, NPS loss, OBJ loss, and CSS loss, to obtain the optimal adversarial patch. Algorithm 1 illustrates the complete procedure for the MVPatch algorithm.

where $\mathcal{L}$ represents the cross-entropy loss function. To solve the optimization problem, we can utilize the Adam optimizer, which is one of the most common and widely used optimization techniques.

B. Threat Models

We apply the YOLOv2, YOLOv3, YOLOv3-tiny, YOLOv4, and YOLOv4-tiny models to generate adversarial patches. These patches are then evaluated on the YOLOv5, Faster-RCNN, and SSD models to assess their transferability in attacks. In the object context of the YOLO series, given the benign image $\mathcal{I}$, the objective of the adversarial attack is to jeopardize the object detector $f_\theta(x, \mathcal{Y})$, where x belongs to $\mathcal{I}$, $\mathcal{Y} = \{\mathrm{a, b, w, h, obj, cls}\}$ and θ denotes the parameter of the object detector. We suppress the object confidence score by utilizing the adversarial patches. a and b are represented by the value of the horizontal and vertical coordinates of the detection frame. w and h are the width and height of the detection frame. obj and cls are object confidence scores and classification scores. Our focus is to suppress the person's object confidence score by optimizing the use of adversarial patches.

C. Robustness of Adversarial Patch in the Physical Domain

Previous studies have primarily focused on applying adversarial patches in the digital domain. However, it is important to recognize that adversarial patches can also appear in the physical domain. To enhance the effectiveness of adversarial patches in physical attacks, we propose the utilization of the Non-Printable Score (NPS) [28] and Total-Variation (TV) [3] as loss functions. These will aid in the creation of more aggressive and robust adversarial patches specifically designed for physical scenarios. We present the NPS for improving the robustness when we generate adversarial patches in the physical domain using digital patterns and to ensure compatibility with the iPad

color gamut and printer gamut. The formulation of the NPS is as follows:

$$\mathcal{L}_{\mathrm{NPS}} = \sum_{c \in \mathcal{C}, p \in \mathcal{P}} |p - c|, \tag{4}$$

where $\mathcal{P}$ and $\mathcal{C}$ represent the pixel values of the adversarial patch and the colors that the iPad can display, respectively. Both p and c are elements of $\mathcal{P}$ and $\mathcal{C}$. To improve the physical robustness of adversarial patches, we utilize the Euclidean distance $|\cdot|$ to constrain the generation of adversarial patches.

We also introduce the TV term, which enhances the smoothness of neighboring pixels. The TV formulation is defined as:

$$\mathcal{L}_{\mathrm{TV}} = \sum_{a,b} |p_{a,b} - p_{a,b+1}| + |p_{a,b} - p_{a+1,b}|, \tag{5}$$

where p denotes the pixel values of the image, while a and b represent the abscissa and ordinate values of a single pixel, respectively.

D. Human-perception-based Method

There is a trade-off between the naturalness and attack performance of adversarial patches. For instance, if an adversarial patch exhibits higher attack performance, it tends to have lower naturalness. In other words, as the similarity to the source image decreases, the success rate of the attack increases. To obtain a more natural adversarial patch, we propose the human-perception-based method by utilizing the Minkowski distance as a loss function to constrain the naturalness of the patch, which we refer to as the Compared Specified Image Similarity (CSS) measurement. The CSS is formulated as follows:

$$\mathcal{L}_{\mathrm{CSS}} = \left(\sum_{i=1}^{N} |\hat{x}_i - x_i|^p \right)^{\frac{1}{p}}, \tag{6}$$

where $\hat{x}$ represents the adversarial patch generated using the specified image x. We choose $p = 2$ in this work and i represents the number of pixels of $\hat{x}_i$ and x_i.

E. Model-perception-based Method

To improve the transferability of adversarial patches, we propose the model-perception-based method. First, we present the use of two distinct loss functions to attack object detection models, as shown below:

$$\mathcal{L}_{\mathrm{OBJ}_1} = \frac{1}{N} \sum_{i=1}^{N} S^i_{\mathrm{OBJ}}(\mathcal{I}^*, \theta), \tag{7}$$

$$\mathcal{L}_{\mathrm{OBJ}_2} = \max_{\mathcal{I}^*}(\{S^i_{\mathrm{OBJ}}(\mathcal{I}^*, \theta)\}_{i=1}^{N}), \tag{8}$$

where S^i_{OBJ} denotes the object confidence score of the ith object detection model in the ensemble of object detection models (YOLOv2, YOLOv3, YOLOv3-tiny, YOLOv4, YOLOv4-tiny). $\mathcal{I}^*$ is the image with adversarial patch and θ corresponds to the parameters of the object detection model.

We compare the attack performance of diverse object confidence score loss functions on various object detection models. It is observed that the adversarial patch generated by $\mathcal{L}_{\mathrm{OBJ}_1}$ outperforms the one generated by $\mathcal{L}_{\mathrm{OBJ}_2}$ in terms of attacking the object detection model. The adversarial patches generated through diverse loss functions are then applied to eight object detection models (Faster-RCNN, SSD, YOLOv2, YOLOv3, YOLOv3-tiny, YOLOv4, YOLOv4-tiny, and YOLOv5 models) to assess their attack performance and similarity to specified images. The adversarial patch generated by $\mathcal{L}_{\mathrm{OBJ}_1}$ not only exhibits excellent attack capability (the average mAP of $\mathcal{L}_{\mathrm{OBJ}_1}$ is 32.20% and the average mAP of $\mathcal{L}_{\mathrm{OBJ}_2}$ is 51.80%) but also maintains a high level of naturalness. Consequently, we select $\mathcal{L}_{\mathrm{OBJ}_1}$ as our objective loss function. The results of the experiment are illustrated in Table I, where the Faster-RCNN, SSD, YOLOv2, YOLOv3, YOLOv3-tiny, YOLOv4, YOLOv4-tiny, and YOLOv5 models are included as threat models. The mean mAP represents the average value of the mean Average Precision (mAP) obtained from diverse models. CS corresponds to the Cosine Similarity and ED denotes the Euclidean Distance.

F. Dual-perception-based Framework to Generate MVPatch

To make the optimization process converge faster, we introduce additional optimization factors to the previously mentioned loss functions and formulate an ensemble loss function as Equation (9):

$$\mathcal{L}_{\mathrm{TOTAL}} = \alpha\mathcal{L}_{\mathrm{NPS}} + \beta\mathcal{L}_{\mathrm{TV}} + \lambda\mathcal{L}_{\mathrm{CSS}} + \mathcal{L}_{\mathrm{OBJ}}. \tag{9}$$

Since optimizing the ensemble loss function with the Adam optimizer is challenging, we modified our optimization strategy. Instead of reducing the learning rate as training epochs increase, we set thresholds for the parameters and decrease the learning rate when a parameter no longer exhibits optimization during the training process. The updating strategy for the learning rate is governed by Equation (10):

$$\mathcal{LR}_{\mathrm{N}} = \gamma\mathcal{LR}_{\mathrm{O}}, \tag{10}$$

where $\mathcal{LR}_{\mathrm{N}}$ is the new learning rate, while $\mathcal{LR}_{\mathrm{O}}$ corresponds to the old learning rate. In our experiments, we utilize $\gamma = 0.01$ as the decay coefficient.

The complete process is summarized in Algorithm 1. This algorithm aims to generate an adversarial patch, referred to as MVPatch, for a given original image $\mathcal{I}$ using a neural network $f(x)$ with the output being the adversarial patch $\mathcal{P}$.

Algorithm 1 Generating Adversarial Patch (MVPatch)

1: **Input:** Original Image $\mathcal{I}$, Neural Network $f(x)$
2: **Output:** Adversarial Patch $\mathcal{P}$
3: Initialize patch mask $\mathcal{M}$
4: Initialize patch $\mathcal{P}$ using $\mathcal{M}$
5: $\mathcal{I}^* = (1 - \mathcal{M}) \odot \mathcal{I} + \mathcal{M} \odot \mathcal{P}$
6: $\mathcal{L}_{\mathrm{TOTAL}} \leftarrow \alpha\mathcal{L}_{\mathrm{NPS}} + \beta\mathcal{L}_{\mathrm{TV}} + \lambda\mathcal{L}_{\mathrm{CSS}} + \mathcal{L}_{\mathrm{OBJ}}$
7: Initialize learning rate $\mathcal{LR}$ and epochs E
8: **while** not converged or $E < E_{\mathrm{MAX}}$ **do**
9:     Update $\mathcal{I}^*$ using backpropagation based on $\mathcal{L}_{\mathrm{TOTAL}}$
10:     Update patch mask $\mathcal{M}$ based on $\mathcal{I}^*$
11:     Update patch $\mathcal{P}$ based on $\mathcal{M}$
12:     $E \leftarrow E + 1$
13:     **if** parameter optimization threshold not reached **then**
14:         $\mathcal{LR} \leftarrow \gamma$
15:     **end if**
16: **end while**
17: **Return:** Adversarial Patch P

IV. EXPERIMENTS

In this section, we briefly introduce the environment and dataset in the experiment. Additionally, we propose evaluation metrics for the experiment. In the digital environment, we generate meaningful and meaningless adversarial patches and compare them with similar patch attack approaches. In the physical environment, we compare the Attack Success Rate (ASR) of MVPatch with similar patch attack methods and vary the angles and distances between the patch and camera to investigate their impacts on the ASR.

A. Implementation Details

In the digital setting, we initialize the adversarial patch using Gaussian noise. We then segment the patch mask onto the person image and overlay the adversarial patch onto the mask. Finally, we input the image with the adversarial patch into the object detection model. The threat models considered in our experiments are YOLOv2, YOLOv3, YOLOv3-tiny, YOLOv4, and YOLOv4-tiny. For evaluating the transferability of the attack, we utilize YOLOv5, Faster-RCNN, and SSD as the transferable attack models. Subsequently, we calculate the loss functions, including $\mathcal{L}_{\mathrm{OBJ}}$, $\mathcal{L}_{\mathrm{NPS}}$, $\mathcal{L}_{\mathrm{CSS}}$, and $\mathcal{L}_{\mathrm{TV}}$. To optimize the overall loss function $\mathcal{L}_{\mathrm{TOTAL}} = \alpha\mathcal{L}_{\mathrm{NPS}} + \beta\mathcal{L}_{\mathrm{TV}} + \lambda\mathcal{L}_{\mathrm{CSS}} + \mathcal{L}_{\mathrm{OBJ}}$ using backpropagation and the Adam optimizer, we set parameters as $\alpha = 0.01$, $\beta = 2.5$, and $\lambda = 2.5$.

In the physical setting, we employ YOLOv2 as the experimental model to evaluate the Attack Success Rate (ASR) of the generated patches. The parameters of YOLOv2, including $\mathrm{Conf}_{\mathrm{THRESHOLD}} = 0.75$ and $\mathrm{NMS}_{\mathrm{THRESHOLD}} = 0.5$, are carefully selected. For collecting the source images, we utilize the iPhone 11 camera, which serves as our image input device.

TABLE I
ATTACK PERFORMANCE AND COMPREHENSIVE EVALUATION WITH DIVERSE OBJECTIVE LOSS FUNCTIONS

	Faster-RCNN	SSD	YOLOv2	YOLOv3	YOLOv3-tiny	YOLOv4	YOLOv4-tiny	YOLOv5	Mean mAP	CS	ED
$\mathcal{L}_{\mathbf{OBJ}_1}$	**42.07%**	**54.57%**	**30.26%**	**31.39%**	**13.49%**	**27.31%**	**22.74%**	**35.72%**	**32.20%**	**97.91%**	**0.0428**
$\mathcal{L}_{\mathbf{OBJ}_2}$	49.40%	61.08%	50.34%	37.47%	41.44%	52.64%	56.46%	56.46%	51.80%	97.91%	0.0419

B. Experimental Environment and Dataset

For training and evaluating the proposed approach, we utilize the Inria Person dataset [59], which is specifically designed for pedestrian detection tasks. The dataset comprises 614 images for training and 288 images for testing. We utilize an RTX 3090 for the computational module and a 12* Xeon Platinum 8260C for task scheduling. Python version 3.6 and PyTorch version 1.6.1 are used.

In the digital setting, we evaluate the performance of the proposed approach using meaningful adversarial patches and meaningless adversarial patches. These patches are added to images of people from the Inria dataset.

In the physical setting, we print the generated MVPatch using an iPad and attach it to the chest of the investigator. By varying the angles ($0°$, $30°$, $60°$, $90°$) and distances (1 meter, 2 meters, 3 meters, 4 meters) between the human and the camera, we investigate the attack performance of MVPatch and other similar attack methods in a physical setting.

C. Evaluation Metrics

To evaluate the naturalness and attack transferability of MVPatch, we employed the following evaluation metrics: mean Average Precision (mAP), Naturalness Score (NS), and Transferability Score (TS).

mAP (mean Average Precision): The mAP is a widely used metric calculated by summing the average precision of models for each test sample and dividing it by the total number of test samples. It allows for comparisons of model performance across different datasets. The precision 'PREC' is computed as the ratio of true positive samples divided by the sum of true positive and false positive samples. The recall 'REC' is calculated as the ratio of true positive samples divided by the sum of true positive and false negative samples. Formally,

$$\text{PREC} = \frac{\text{TP}}{\text{TP} + \text{FP}}, \quad \text{REC} = \frac{\text{TP}}{\text{TP} + \text{FN}},$$
$$\text{mAP} = \frac{1}{n-1} \sum_{i=1}^{n-1} (\text{REC}_{i+1} - \text{REC}_i)\text{PREC}_{i+1}, \quad (11)$$

where TP, FP, TN, and FN denote respectively true positive sample, false positive sample, true negative sample, and false negative sample. Through the equation mentioned above, we can obtain the mAP of the object detection models.

NS (Naturalness Score): The NS is used to measure the similarity between the adversarial patch and the specified image, which is defined as

$$\text{NS} = \lambda \left(\frac{\text{CSS} - \widehat{\text{CSS}}_{\text{NG}}}{\widehat{\text{CSS}}_{\text{S}} - \widehat{\text{CSS}}_{\text{NG}}} + \frac{\text{CSS} - \widehat{\text{CSS}}_{\text{NR}}}{\widehat{\text{CSS}}_{\text{S}} - \widehat{\text{CSS}}_{\text{NR}}} \right)$$
$$+ (1 - \lambda) \left(\frac{\text{ED} - \widehat{\text{ED}}_{\text{NG}}}{\widehat{\text{ED}}_{\text{NG}} - \widehat{\text{ED}}_{\text{S}}} + \frac{\text{ED} - \widehat{\text{ED}}_{\text{NR}}}{\widehat{\text{ED}}_{\text{NR}} - \widehat{\text{ED}}_{\text{S}}} \right), \quad (12)$$

where CSS represents the cosine similarity score between the specified image and adversarial patch and $\widehat{\text{CSS}}$ is the cosine similarity score between the specified image and adversarial patch of NG and NR images. ED denotes the Euclidean distance. NG and NR are gray-scale and random noise. S is an abbreviation for the source image. A higher naturalness score indicates that MVPatch has a stronger similarity to the specified image.

TS (Transferability Score): The TS measures the transferable attack performance of the adversarial patch across diverse object detection models, which is defined as

$$\text{TS} = \frac{1}{N} \sum_{i=0}^{N} \left(\frac{\|D_i - \widehat{D}_i^{\text{NG}}\|_2}{\widehat{D}_i^{\text{NG}}} + \frac{\|D_i - \widehat{D}_i^{\text{NR}}\|_2}{\widehat{D}_i^{\text{NR}}} \right), \quad (13)$$

where D_i denotes the mAP of object detection models detecting normal images while $\widehat{D}_i$ represents the mAP of object detection models detecting NG and NR images. NG and NR represent gray-scale and random noise. $\| \cdot \|_2$ is the L2 norm to constrain the distances between D_i and $\widehat{D}_i$. The higher transferability score reveals that the adversarial patch has a higher transferable attack performance. We define

$$\text{ASR} = \frac{1}{|\mathcal{D}_{\text{test}}|} \sum_{\mathcal{I} \in \mathcal{D}_{\text{test}}} \mathbb{1}\{f(\mathcal{I}^*, \theta) \neq f(\mathcal{I}, \theta)\}, \quad (14)$$

as an indicator of the attack success rate, where $f(\cdot)$ represents the consequence of the models' detection. $\mathcal{D}_{\text{test}}$ denotes a set of benign images from test datasets. The ASR equals 1 when $f(\mathcal{I}^*, \theta) \neq f(\mathcal{I}, \theta)$, and equals 0 otherwise.

V. RESULTS

This section presents empirical evidence that showcases the effectiveness of the proposed MVPatch through comprehensive evaluations conducted in both digital and physical domains. In the digital domain, we divided the experimental objects into meaningful adversarial patches and meaningless adversarial patches. In the physical domain, we assessed the patch attack performance from various angles and distances by utilizing a camera to capture images as input sources. The experimental results demonstrate that our method outperforms other similar adversarial patch attack methods, both in the digital and physical domains. In the last, we show the visual consequence of the experiment in the digital domain and physical domain.

A. Evaluation of Naturalness in the Digital World

To assess the naturalness of the adversarial patch, we utilize the YOLO series models as threat models. The natural factor, represented by the parameter λ, is adjusted within the range of [1,3] to generate a variety of adversarial patches. The naturalness score (NS) is then calculated to quantify the naturalness of these patches. The generated adversarial patches with different naturalness scores are displayed in Fig.3. As we move from left to right on the coordinate axis, the naturalness score gradually increases, indicating a higher level of naturalness.

TABLE II
EXPERIMENTAL CONSEQUENCE OF NATURALNESS OF MVPATCH

Adversarial Patches	Evaluation Metrics			
	mAP	CS	ED	NS
SRC	65.70%	100%	0.00	100.00
NoiseGrey	74.05%	97.45%	6.01	0.00
NoiseRandom	75.09%	92.82%	8.27	0.00
$\lambda = 1$	32.30%	97.61%	4.63	35.59
$\lambda = 1.25$	32.19%	97.87%	4.24	42.11
$\lambda = 1.5$	34.39%	98.54%	3.73	56.77
$\lambda = 1.75$	33.13%	98.78%	3.44	62.48
$\lambda = 2$	33.98%	99.01%	3.12	68.14
$\lambda = 2.25$	37.49%	99.20%	2.82	72.97
$\boldsymbol{\lambda = 2.5}$	**36.63%**	**99.30%**	**2.53**	**76.08**
$\lambda = 2.75$	37.46%	99.38%	2.21	78.94
$\lambda = 3$	39.69%	99.44%	1.99	81.01

Explanation for Experimental Consequence: $\lambda = [1,3]$ represents the adversarial patches generated by diverse natural factors. SRC represents the source image. NoiseGrey and NoiseRandom are matrices with values of 0.5 and random values, respectively. We deploy the mAP (mean Average Precision), CS (Cosine Similarity), and ED (Euclidean Distance) to measure the attack performance and the similarity of the adversarial patch with the source image.
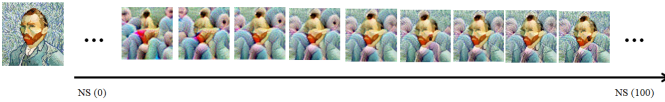

Fig. 3. The naturalness score (NS) of adversarial patches with diverse λ parameters. As the NS increases, the level of similarity between the source image and the generated image rises.

Analysis and Conclusion for Experimental Consequence: As shown in Table II, we vary λ from 1 to 3, resulting in an increase in the score of naturalness from 35.59 to 81.01. Simultaneously, the mAP increases from 32.30% to 39.69%. However, a higher mAP generally corresponds to greater accuracy of the object detection models and a lower attack performance of adversarial patches. There is a tradeoff between naturalness and attack performance, so it is not possible to obtain an adversarial patch with both higher naturalness and attack performance. We identify a threshold for the score of

naturalness that helps us obtain the optimal adversarial patch with both naturalness and attack performance. Through an analysis of 20 experimental participants, it is generally agreed that when the score of naturalness is above 75 ($\lambda = 2.5$), the generated adversarial patch would be considered more natural. Furthermore, if we continue to increase the natural factor λ, the gain in naturalness recognizable to the human eye will decrease. Therefore, we define $\lambda = 2.5$ as the parameter of the loss function in the following experiments. The images with different scores of naturalness for the adversarial patches are shown in Fig.3.

B. Evaluation of Attack Transferability in the Digital domain

To systematically investigate the attack performance of adversarial patches in the digital domain, we divide the experimental objects into two parts: meaningful adversarial patches and meaningless adversarial patches. Most research mainly focused on meaningless adversarial patches and few researchers investigated the meaningful and meaningless adversarial patches in the digital and physical domains.

1) Evaluation of Attack Transferability of Meaningful Adversarial Patches in the Digital domain: We utilize the pre-trained models including YOLOv2, YOLOv3, YOLOv3-tiny, YOLOv4, and YOLOv4-tiny to generate diverse adversarial patches with meaningful content using the natural factor $\lambda = 2.5$, as shown in Fig.4(a), 4(b), 4(c), 4(d), and 4(e). By combining these pre-trained models, we obtain ensemble attack adversarial patches, as shown in Fig.4(f) and 4(n). To compare the influence of person images and other images as adversarial patches for the object detection models, we use the sunflower image (Fig.4(n)) as a control test for the person image (Fig.4(f)). We input all the acquired adversarial patches into transfer attack models, including Faster R-CNN, SSD, YOLOv2, YOLOv3, YOLOv3-tiny, YOLOv4, YOLOv4-tiny, and YOLOv5, to calculate the transferability score and compare it with the Natural Patch [1]. The comparable experimental results are shown in Table III.

Explanation for Experimental Consequence: YOLOv2, YOLOv3, YOLOv3-tiny, YOLOv4, YOLOv4-tiny, YOLOv5, Faster R-CNN, and SSD are pre-trained object detection models. The "Threat Models" column represents diverse adversarial patches generated by different models, including YOLOv2, YOLOv3, YOLOv3-tiny, YOLOv4, YOLOv4-tiny, and the Ensemble Model, which combines YOLOv2, YOLOv3, YOLOv3-tiny, YOLOv4, and YOLOv4-tiny. The "original image" refers to an image without an adversarial attack."Grey-scale Noise" and "Random Noise" separately indicate an image with padding of a value of 0.5 and an image with random values. The Black Box (TS) measures the transferability of adversarial attacks, with the transferability score (TS) indicating superior performance with a higher score.

Evaluation and Analysis for Experimental Consequence: Firstly, we compare the transferability score of MVPatch (Ours) to that of Natural Patch [1] on individual object detection models. MVPatch performs better than Natural Patch on most of the models in the experiment. For the YOLOv4 model,

TABLE III
EXPERIMENTAL CONSEQUENCE OF TRANSFERABILITY OF MEANINGFUL ADVERSARIAL PATCHES (MAP %)

$(Meaningful Adversarial Patches)$ Threat Models	Transfer Attack Models								Black Box(TS ↑)
	Faster RCNN	SSD	YOLOv2	YOLOv3	YOLOv3-tiny	YOLOv4	YOLOv4-tiny	YOLOv5	
(Fig.4(a)) YOLOv2 [Ours]	55.75	63.30	32.28	60.37	29.93	59.98	51.79	62.80	20.22
(Fig.4(i)) YOLOv2 [1]	56.60	56.66	37.96	56.85	58.04	67.74	67.43	66.85	15.21
(Fig.4(b)) YOLOv3 [Ours]	50.81	60.53	50.55	55.44	41.54	52.80	56.79	61.49	27.93
(Fig.4(j)) YOLOv3 [1]	55.35	51.15	49.44	55.39	52.10	66.97	67.09	58.69	23.53
(Fig.4(c)) YOLOv3-tiny [Ours]	59.77	67.39	59.92	69.63	5.31	71.32	62.45	74.66	21.14
(Fig.4(k)) YOLOv3-tiny [1]	52.81	51.55	48.75	63.26	38.99	62.59	65.93	64.11	24.9
(Fig.4(d)) YOLOv4 [Ours]	47.32	56.91	44.96	52.04	15.35	27.89	46.37	45.11	43.69
(Fig.4(l)) YOLOv4 [1]	57.70	60.91	58.73	66.08	69.39	72.64	71.13	75.76	10.76
(Fig.4(e)) YOLOv4-tiny [Ours]	60.85	66.16	49.25	68.07	47.26	72.87	29.53	71.32	22
(Fig.4(m)) YOLOv4-tiny [1]	54.64	41.15	39.90	50.28	31.39	61.88	57.45	54.61	34.41
(−) **Ensemble Model [1]**	**61.28**	**52.28**	**49.42**	**35.46**	**25.29**	**51.71**	**18.51**	**64.00**	**40**
(Fig.4(n)) **Ensemble Model [Ours]**	**45.96**	**55.52**	**32.09**	**25.66**	**21.69**	**36.43**	**28.74**	**35.36**	**52.82**
(Fig.4(f)) **Ensemble Model [Ours]**	**42.07**	**54.57**	**30.26**	**31.39**	**13.49**	**27.31**	**22.74**	**35.72**	**56.83**
(Fig.4(g),4(o)) Srouce Image	60.66	66.76	58.60	68.59	57.04	68.78	70.08	75.07	0
(Fig.4(h)) Grey-scale Noise	61.75	72.05	67.75	76.22	80.69	75.22	76.89	81.86	0
(Fig.4(p)) Random Noise	63.70	73.19	69.67	75.37	82.36	75.79	78.95	81.69	0

(a) (b) (c) (d) (e) (f) (g) (h)
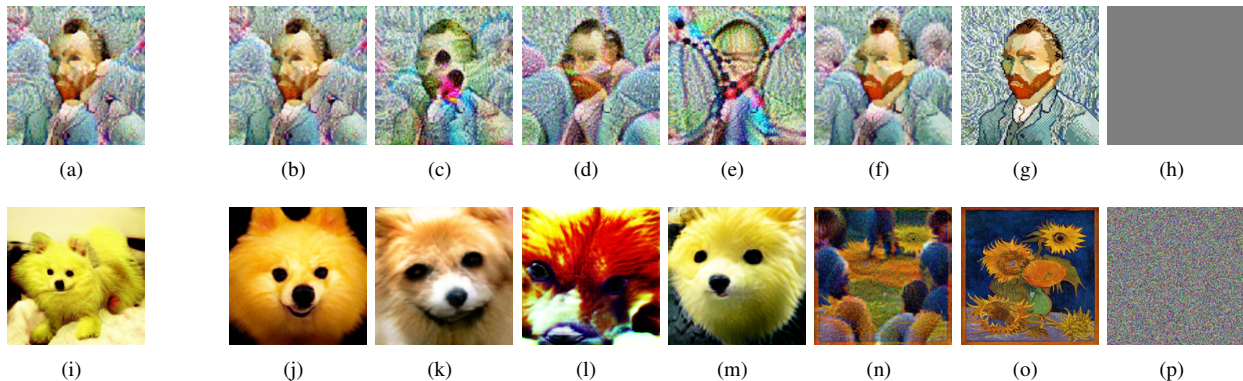
(i) (j) (k) (l) (m) (n) (o) (p)

Fig. 4. Adversarial patches are generated by various object detectors, including YOLOv2, YOLOv3, YOLOv3-tiny, YOLOv4, and YOLOv4-tiny and compared attack performance on the individual model with Natural Patch [1]. Additionally, we compare the performance of our ensemble attack with that of the Natural Patch. The attack performance of diverse adversarial patches are illustrated as Table III.

the TS of MVPatch is approximately 33% higher than the TS of Natural Patch. Similarly, the excellent attack performance of MVPatch is observed on the other four object detection models (YOLOv2, YOLOv3, YOLOv3-tiny, and YOLOv4-tiny). On the other hand, the attack performance of MVPatch on the ensemble model is surpassed by Natural Patch, with the TS of MVPatch on the ensemble model being approximately 16% higher than the TS of Natural Patch.

From the results of the meaningful adversarial patch experiment, it can be seen that the proposed algorithm for meaningful adversarial patches, MVPatch, achieves superior performance compared to the similar algorithm, Natural Patch, in terms of attack transferability.

2) Evaluation of Attack Transferability of Meaningless Adversarial Patches in the Digital domain: We adjust the natural factor of $\lambda = 0$ and utilize the joint pre-trained models, including YOLOv2, YOLOv3, YOLOv3-tiny, YOLOv4, and YOLOv4-tiny, to generate meaningless adversarial patch

MVPatch. In comparison, we consider AdvPatch [2], Adv-Texture [3], and AdvCloak [32] as subjects for the experiment on meaningless adversarial patches. We use all the obtained adversarial patches as input for Faster R-CNN, SSD, YOLOv2, YOLOv3, YOLOv3-tiny, YOLOv4, YOLOv4-tiny, and YOLOv5, calculate the transferability scores, and compare them with those of AdvPatch [2], AdvTexture [3], and Adv-Cloak [32]. The comparable experimental results are presented in TableIV.

Explanation for Experimental Consequence: YOLOv2, YOLOv3, YOLOv3-tiny, YOLOv4, YOLOv4-tiny, YOLOv5, Faster R-CNN, and SSD are pre-trained object detection models. The "Meaningless Adversarial Patches" column represents various meaningless adversarial patches generated by diverse attack algorithms. The Black Box (TS) measures the transferability of adversarial attacks, with a higher transferability score indicating better performance. TS stands for the transferability score.

TABLE IV
EXPERIMENTAL CONSEQUENCE OF TRANSFERABILITY OF MEANINGLESS ADVERSARIAL PATCHES (MAP %)

Meaningless Adversarial Patches	Transfer Models								Black Box(TS↑)
	Faster-RCNN	SSD	YOLOv2	YOLOv3	YOLOv3-tiny	YOLOv4	YOLOv4-tiny	YOLOv5	
AdvPatch [2]	43.11	48.57	4.69	47.59	34.24	58.74	33.82	49.65	46.29
AdvTexture [3]	48.18	36.12	5.31	46.83	18.74	63.03	34.13	60.47	47.56
AdvCloak [32]	55.19	60.82	33.74	54.77	53.42	67.57	56.12	68.05	24.62
MVPatch[Ours]	**34.95**	**48.95**	**23.93**	**13.09**	**6.04**	**26.72**	**14.77**	**34.35**	**64.47**

TABLE V
EXPERIMENTAL CONSEQUENCE OF MVPATCH AND OTHER PATCHES IN THE PHYSICAL DOMAIN

Adversarial Patches	Evaluation Metrics					
	ASR	Number of Images	Stealthiness Attack	Physical Attack	Transferable Attack	Lightweight Model
(Fig.5(a))AdvPatch [2]	13.57%	1319	×	✓	×	✓
(Fig.5(b))AdvTexture [3]	12.72%	1211	×	✓	×	×
(Fig.5(c))Benign Image	5.03%	1194	✓	×	×	×
(Fig.5(d))Natural Patch [1]	8.32%	1646	✓	✓	✓	×
(Fig.5(e))Natural Patch [1]	19.43%	1616	✓	✓	✓	×
(Fig.5(f))**MVPatch [Ours]**	**22.60%**	**1438**	✓	✓	✓	✓
(Fig.5(g))**MVPatch [Ours]**	**26.33%**	**1257**	✓	✓	✓	✓

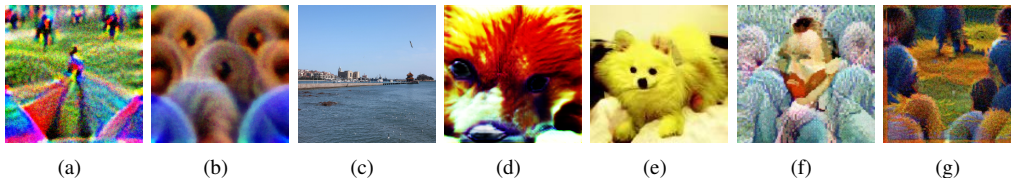| (a) | (b) | (c) | (d) | (e) | (f) | (g) |

Fig. 5. Adversarial patches, such as AdvPatch [2], AdvTexture [3], Natural Patch [1], and our MVPatch, are employed in the physical world using diverse attack methods. TableV displays the attack success rate of different adversarial patches, as well as other important evaluation metrics.

Evaluation and Analysis for Experimental Consequence: As illustrated in Table IV, the transferability score (TS) of MVPatch is approximately 40% higher than that of Adv-Cloak. Compared to AdvPatch and AdvTexture, the TS of MVPatch is approximately 20% higher. Moreover, when the transfer models, including YOLOv2, YOLOv3, YOLOv3-tiny, YOLOv4, YOLOv4-tiny, YOLOv5, Faster R-CNN, and SSD, are attacked by MVPatch, their mean Average Precision (mAP) reduces by 10 to 20%, compared to the other three algorithms.

To sum up, in terms of meaningless adversarial patches, the proposed algorithm, MVPatch, exhibits higher attack transferability compared to similar algorithms.

C. Evaluation of Attack Performance of Adversarial Patches in the Physical domain

To systematically investigate the attack performance of adversarial patches in the physical domain, we divide the experimental conditions into two parts: diverse angles and diverse distances. Prior research mainly focused on the attack performance of adversarial patches in the physical domain and few researchers investigated how impact the attack performance of adversarial patches using diverse angles and distances.

1) Evaluation of Attack Performance of Diverse Adversarial Patches in the Physical Domain: The volunteers hold various adversarial patches, including AdvPatch, AdvTexture, a benign image, Natural Patch, and the proposed MVPatch, against their chests. The patches are positioned at an angle of $\{0°, 30°, 60°, 90°\}$ and a distance of $\{1, 2, 3, 4\}$ meters. We use an iPhone 11 to capture the images with the adversarial patches from diverse distances and angles in the physical world. In total, we collected 9681 images. To preserve the pixel details of the adversarial patches, we view them using an iPad Pro. The attack success rates and some evaluation metrics of different adversarial patches are shown in Table V, and sample patches are displayed in Fig.5.

Explanation for Experimental Consequence: The AdvPatch [2], and AdvTetxure [3] are both meaningless adversarial patches and the Natural Patches [1] and proposed MVPatches are meaningful patches. The Benign Image refers to an image without adversarial examples. ASR is short for attack success rate. Number of Images represents the number of experimental images to evaluate the attack performance. Stealthiness Attack means that the attack has a more naturalness score. Physical Attack denotes that the attack can be applied in the physical world. Transferable Attack represents that the attack has transferable attack ability. A lightweight model means that
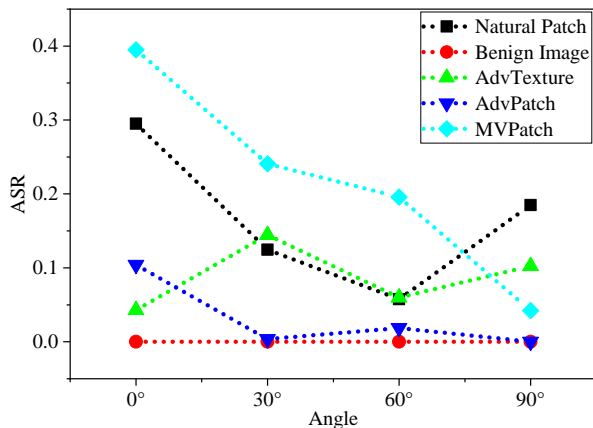
(a) Impact of diverse angles to ASR of adversarial patches
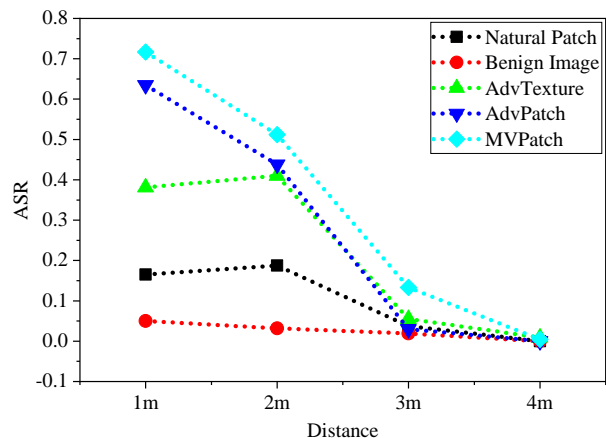
(b) Impact of diverse distances to ASR of adversarial patches

Fig. 6. Experimental consequence illustration of the adversarial patches attacking in the physical domain. Fig.6(a) illustrates the impact of varying camera angles on the ASR of different attack methods, such as Natural Patch, AdvPatch, AdvTexture, Benign Image, and MVPatch. Fig.6(b) illustrates the impact of varying distances between the camera and patches on the ASR of different attack methods, such as Natural Patch, AdvPatch, AdvTexture, Benign Image, and MVPatch.

the model, that generates the adversarial patches, has low computational cost.

Evaluation and Analysis for Experimental Consequence: As Table V illustrates, both AdvPatch(Fig.5(a)) and AdvTetxure(Fig.5(b)) do not have much more attack performance on the YOLOv2 model in the physical world and the ASRs are 13.57% and 12.72%, respectively. The Natural Patch(Fig.5(e)) has higher ASR and its value of ASR is 19.43%, but the other Natural Patch(Fig.5(d)) does not perform as well as Fig.5(e). The ASR of the first Natural Patch(Fig.5(d)) is almost close to the Benign Image(Fig.5(c)). The MVPatches perform better than other adversarial patches in the physical world. The ASR of MVPatches are respectively 22.60% (Fig.5(f)) and 26.33% (Fig.5(g)). Consequently, we ensure the MVPatch has more attack performance than others in the physical world.

2) Evaluation of Attack Performance from Diverse Angles in the Physical Domain: We collected 6846 images from various angles ($0°$, $30°$, $60°$, $90°$) to assess the impact of different angles on the attack performance of adversarial patches, including the Natural Patch, AdvPatch, AdvTexture, Benign Image, and our MVPatch. To keep the fairness of the experiment, we change angles from $\{0°, 30°, 60°, 90°\}$ with the same distance (2 meters). The volunteer rotated while the adversarial patch rotated in the opposite direction, ensuring that the patch always faced the camera. We refer to this setup as "with Rotation". The experimental results are presented in Fig.6(a).

Explanation for Experimental Consequence: The light blue dotted line with squares represents the MVPatch with Rotation, while the red dotted line with circles represents the Benign Image with Rotation. The dark blue dotted line with triangles represents the AdvPatch with Rotation, while the green dotted line with triangles represents the AdvTexture with Rotation. The black dotted line with squares represents the Natural Patch with Rotation. The X-axis represents the angles, while the Y-axis represents the attack success rate.

Evaluation and Analysis for Experimental Consequence:

The effectiveness of adversarial patches with rotation diminishes as the angle of rotation increases. At an angle of $0°$, the ASR of the MVPatch can reach 39.5%, and other patches perform well at the angle of $0°$ except for the AdvTexture. At the angle of $90°$, the ASRs of the Natural Patch and AdvTexture surpass the MVPatch at the same angle. Even a slight variation in the angle can significantly enhance the robustness and aggressiveness of the adversarial patch when it is rotated. Fig.6(a) also demonstrates that the MVPatch outperforms other attack methods in terms of angle variations (at the angles of $0°$, $30°$, and $60°$).

3) Evaluation of Attack Performance from Diverse Distance in the Physical Domain: A total of 3984 images are collected at various distances (1 meter, 2 meters, 3 meters, and 4 meters) to assess how different distances impact the attack performance of adversarial patches, specifically MVPatch, Natural Patch, AdvPatch, AdvTexture, and Benign Image. To keep the fairness of the experiment, we change distances from $\{1, 2, 3, 4\}$ meters with the same angle ($0°$). Fig.6(b) presents the results.

Explanation for Experimental Consequence: MVPatch is represented by the light blue dotted line with squares. Natural Patch is represented by the black dotted line with squares. AdvPatch is represented by the dark blue dotted line with triangles. AdvTexture is represented by the green dotted line with triangles. The benign Image is represented by the red dotted line with circles. The X-axis represents the attack success rate, and the Y-axis represents the distance from the volunteer with the adversarial patch to the camera.

Evaluation and Analysis for Experimental Consequence: As Fig.6(b) shows, the adversarial patches generated by MV-Patch and AdvPatch exhibit high levels of aggression when the volunteer is at a distance of one meter from the camera. The ASR of MVPatch is 71.67% and the ASR of AdvPatch is 63.46% at a distance of 1 meter. As the volunteer moves farther away from the camera (beyond one meter), the effectiveness of the attack diminishes. However, the adversarial patches gener-

(a) Benign Images   (b) Malicious Images   (c) Benign Images   (d) Malicious Images   (e) Benign Images   (f) Malicious Image

Fig. 7. Illustration of experimental consequence in the digital domain. The images with green rectangles represent the object detectors can recognize the class of a person successfully while the images with red rectangles denote the object detectors can not recognize the class of a person.

ated by AdvTexture and Natural Patch have higher aggression at a distance of 2 meters. When the volunteer moves farther away from the camera (beyond two meters), the effectiveness of the attack diminishes. Similarly, the attack weakens as the volunteer moves closer.

D. Illustraton of Experimental Consequence

This section provides experimental results in both the digital and physical domains to demonstrate our proposed approach. The green rectangle represents a successful detection of a person by the object detector, while the red rectangle indicates a failure to detect the person class. In the digital domain, we choose various experimental images from the Inria Person dataset as evaluation objects. In the physical domain, the source images of this experiment are not covered with mosaics. For privacy protection, mosaics are later added near the face. Fig.7 displays the results of digital experiments, while Fig.8 depicts the results of physical experiments.

VI. CONCLUSION

In this paper, we propose a dual-perception-based attack framework. This framework comprises a model-perception degradation method and a human-perception improvement method. The aim is to create vivid and aggressive adversarial patches, which we refer to as MVPatch, for person detection models suitable for real-world implementation. In terms of the model-perception degradation method, we exploit the ensemble attack on various object detectors to enhance the transferability of the adversarial patch. In terms of the human-perception improvement method, we introduce a lightweight approach for visual similarity measurement designed to make the adversarial patch less noticeable. Through extensive qualitative and quantitative experiments, we compare different approaches and find that minimizing the object loss yields the most effective patches while maintaining competitive attack performance compared to similar methods. We evaluate the transferability and naturalness of the crafted adversarial
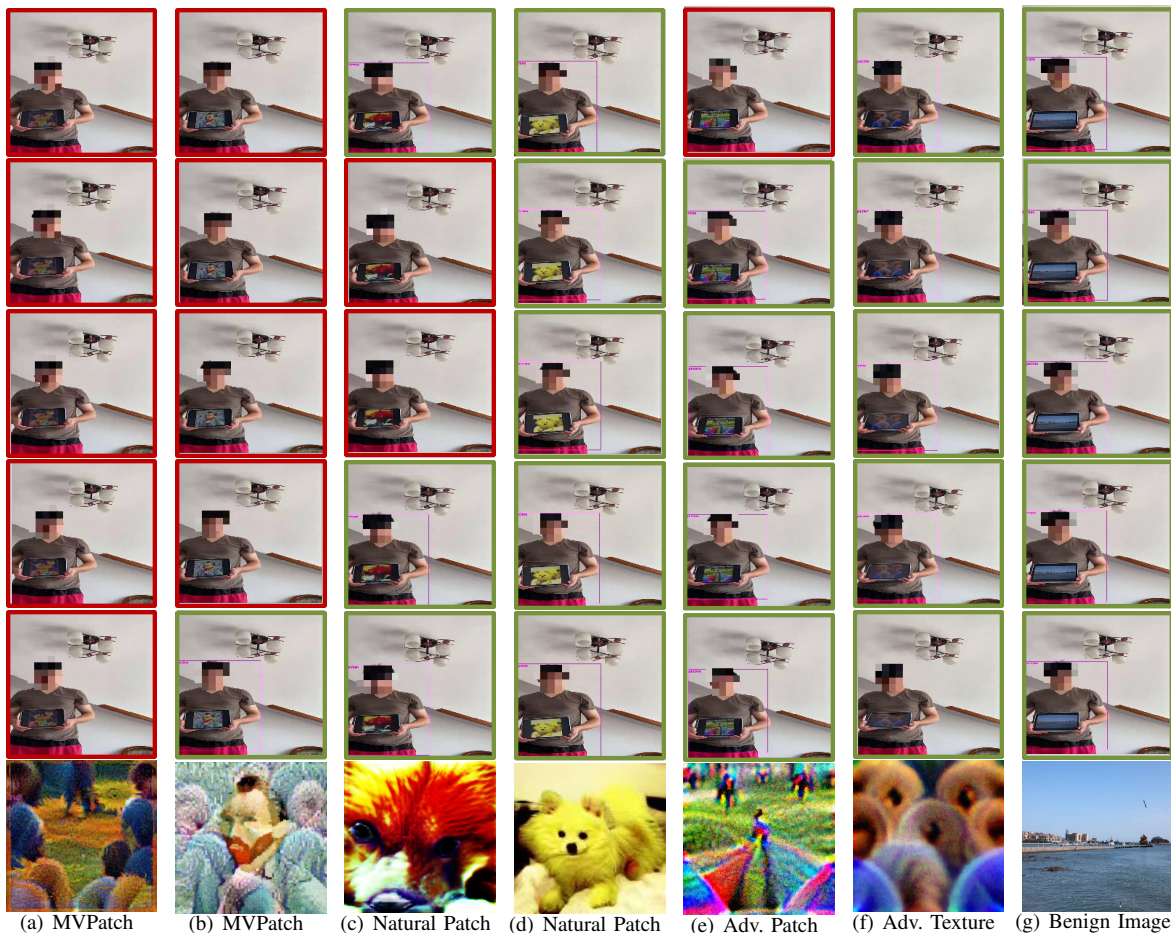
Fig. 8. This illustration demonstrates the experimental outcomes in the physical domain. Images with a green rectangle represent successful recognition of the person's class by the object detectors, whereas images with a red rectangle indicate the object detectors' failure to recognize the person's class. The images at the bottom are adversarial patches and mosaics are added after detection, to avoid privacy disclosure for volunteers.

patches in both digital and physical domains. Extensive experiments demonstrate that the proposed MVPatch performs remarkable stealthiness and transferability with few computational costs.

However, there are still limitations in terms of factors such as angles and distance that can affect the performance of adversarial attacks. In future work, we aim to explore approaches to designing adversarial patches that can minimize the influence of angle and distance and maximize attack performance in both digital and physical domains.

REFERENCES

[1] Y.-C.-T. Hu, J.-C. Chen, B.-H. Kung, K.-L. Hua, and D. S. Tan, "Naturalistic physical adversarial patch for object detectors," in *2021 IEEE/CVF International Conference on Computer Vision*, 2021, pp. 7828–7837.

[2] S. Thys, W. Van Ranst, and T. Goedemé, "Fooling automated surveillance cameras: adversarial patches to attack person detection," in *CVPRW: The Bright and Dark Sides of Computer Vision: Challenges and Opportunities for Privacy and Security*, 2019.

[3] Z. Hu, S. Huang, X. Zhu, X. Hu, F. Sun, and B. Zhang, "Adversarial texture for fooling person detectors in the physical world," *IEEE/CVF Conference on Computer Vision and Pattern Recognition*, pp. 13 297–13 306, 2022.

[4] A. Krizhevsky, I. Sutskever, and G. E. Hinton, "Imagenet classification with deep convolutional neural networks," *Advances in neural information processing systems*, vol. 25, 2012.

[5] W. Wang, J. Shen, and L. Shao, "Video salient object detection via fully convolutional networks," *IEEE Transactions on Image Processing*, vol. 27, no. 1, pp. 38–49, 2017.

[6] K. He, X. Zhang, S. Ren, and J. Sun, "Deep residual learning for image recognition," in *Proceedings of the IEEE Conference on Computer Vision and Pattern Recognition*, 2016, pp. 770–778.

[7] J. Li, H. Chang, J. Yang, W. Luo, and Y. Fu, "Visual representation and classification by learning group sparse deep stacking network," *IEEE Transactions on Image Processing*, vol. 27, no. 1, pp. 464–476, 2017.

[8] I. Sutskever, O. Vinyals, and Q. V. Le, "Sequence to sequence learning with neural networks," *Advances in Neural Information Processing Systems*, vol. 27, 2014.

[9] J. Hirschberg and C. D. Manning, "Advances in natural language processing," *Science*, vol. 349, no. 6245, pp. 261–266, 2015.

[10] A.-r. Mohamed, G. E. Dahl, and G. Hinton, "Acoustic modeling using deep belief networks," *IEEE Transactions on Audio, Speech, and Language Processing*, vol. 20, no. 1, pp. 14–22, 2011.

[11] G. Hinton, L. Deng, D. Yu, G. E. Dahl, A.-r. Mohamed, N. Jaitly, A. Senior, V. Vanhoucke, P. Nguyen, T. N. Sainath, *et al.*, "Deep neural networks for acoustic modeling in speech recognition: The shared views of four research groups," *IEEE Signal Processing Magazine*, vol. 29, no. 6, pp. 82–97, 2012.

[12] C. Szegedy, W. Zaremba, I. Sutskever, J. Bruna, D. Erhan, I. J. Goodfellow, and R. Fergus, "Intriguing properties of neural networks," in *Proceedings of the International Conference on Learning Representations*, vol. abs/1312.6199, 2014.

[13] I. J. Goodfellow, J. Shlens, and C. Szegedy, "Explaining and harnessing adversarial examples," in *Proceedings of the International Conference on Learning Representations*, vol. abs/1412.6572, 2015.

[14] Y. Zhang, X. Tian, Y. Li, X. Wang, and D. Tao, "Principal component

adversarial example," *IEEE Transactions on Image Processing*, vol. 29, pp. 4804–4815, 2020.

[15] X. Wei, Y. Guo, and J. Yu, "Adversarial sticker: A stealthy attack method in the physical world," *IEEE Transactions on Pattern Analysis and Machine Intelligence*, 2022.

[16] X. Wei, Y. Guo, J. Yu, and B. Zhang, "Simultaneously optimizing perturbations and positions for black-box adversarial patch attacks," *IEEE Transactions on Pattern Analysis and Machine Intelligence*, vol. 45, no. 7, pp. 9041–9054, 2023.

[17] Y. Wang, E. Sarkar, W. Li, M. Maniatakos, and S. E. Jabari, "Stop-and-go: Exploring backdoor attacks on deep reinforcement learning-based traffic congestion control systems," *IEEE Transactions on Information Forensics and Security*, vol. 16, pp. 4772–4787, 2021.

[18] X. Yuan, S. Hu, W. Ni, X. Wang, and A. Jamalipour, "Deep reinforcement learning-driven reconfigurable intelligent surface-assisted radio surveillance with a fixed-wing uav," *IEEE Transactions on Information Forensics and Security*, vol. 18, pp. 4546–4560, 2023.

[19] A. Madry, A. Makelov, L. Schmidt, D. Tsipras, and A. Vladu, "Towards deep learning models resistant to adversarial attacks," in *Proceedings of the International Conference on Learning Representations*, 2018.

[20] N. Carlini and D. A. Wagner, "Towards evaluating the robustness of neural networks," in *IEEE Symposium on Security and Privacy*, 2017, pp. 39–57.

[21] S.-M. Moosavi-Dezfooli, A. Fawzi, and P. Frossard, "Deepfool: A simple and accurate method to fool deep neural networks," in *IEEE/CVF Conference on Computer Vision and Pattern Recognition*, 2016, pp. 2574–2582.

[22] A. Kurakin, I. J. Goodfellow, and S. Bengio, "Adversarial examples in the physical world," in *Proceedings of the International Conference on Learning Representations*, Toulon, France, April 2017.

[23] N. Papernot, P. McDaniel, S. Jha, M. Fredrikson, Z. B. Celik, and A. Swami, "The limitations of deep learning in adversarial settings," in *IEEE European Symposium on Security and Privacy*, 2016, pp. 372–387.

[24] P.-Y. Chen, H. Zhang, Y. Sharma, J. Yi, and C.-J. Hsieh, "Zoo: Zeroth order optimization based black-box attacks to deep neural networks without training substitute models," in *ACM Workshop on Artificial Intelligence and Security*, 2017.

[25] P. Neekhara, S. S. Hussain, P. Pandey, S. Dubnov, J. McAuley, and F. Koushanfar, "Universal adversarial perturbations for speech recognition systems," in *Proceedings of the International Speech Communication Association*, 2019, pp. 481–485.

[26] J. Su, D. V. Vargas, and K. Sakurai, "One pixel attack for fooling deep neural networks," *IEEE Transactions on Evolutionary Computation*, vol. 23, pp. 828–841, 2019.

[27] A. Athalye, L. Engstrom, A. Ilyas, and K. Kwok, "Synthesizing robust adversarial examples," in *International Conference on Machine Learning*, 2017.

[28] M. Sharif, S. Bhagavatula, L. Bauer, and M. K. Reiter, "Accessorize to a crime: Real and stealthy attacks on state-of-the-art face recognition," *ACM SIGSAC Conference on Computer and Communications Security*, 2016.

[29] S. A. Komkov and A. Petiushko, "Advhat: Real-world adversarial attack on arcface face id system," in *25th International Conference on Pattern Recognition*, 2020, pp. 819–826.

[30] T. B. Brown, D. Mané, A. Roy, M. Abadi, and J. Gilmer, "Adversarial patch," *arXiv preprint arXiv:1712.09665*, 2017.

[31] X. Liu, H. Yang, Z. Liu, L. Song, H. Li, and Y. Chen, "Dpatch: An adversarial patch attack on object detectors," in *AAAI Workshop on Artificial Intelligence Safety*, Hawaii, USA, Jun 2019.

[32] Z. Wu, S.-N. Lim, L. S. Davis, and T. Goldstein, "Making an invisibility cloak: Real world adversarial attacks on object detectors," in *European Conference on Computer Vision*. Springer, 2020, pp. 1–17.

[33] K. Xu, G. Zhang, S. Liu, Q. Fan, M. Sun, H. Chen, P.-Y. Chen, Y. Wang, and X. Lin, "Adversarial t-shirt! evading person detectors in a physical world," in *European Conference on Computer Vision*. Springer, 2020, pp. 665–681.

[34] H. Huang, Z. Chen, H. Chen, Y. Wang, and K. A. Zhang, "T-sea: Transfer-based self-ensemble attack on object detection," in *IEEE/CVF Conference on Computer Vision and Pattern Recognition*, Vancouver, Canada, June 2023.

[35] J. Wang, A. Liu, Z. Yin, S. Liu, S. Tang, and X. Liu, "Dual attention suppression attack: Generate adversarial camouflage in physical world," in *IEEE/CVF Conference on Computer Vision and Pattern Recognition*, 2021, pp. 8561–8570.

[36] A. Liu, X. Liu, J. Fan, Y. Ma, A. Zhang, H. Xie, and D. Tao, "Perceptual-sensitive gan for generating adversarial patches," in *Proceedings of the AAAI Conference on Artificial Intelligence*, vol. 33, 07 2019, pp. 1028–1035.

[37] H. Xue, A. Araujo, B. Hu, and Y. Chen, "Diffusion-based adversarial sample generation for improved stealthiness and controllability," in *IEEE/CVF Conference on Computer Vision and Pattern Recognition*, Vancouver, Canada, June 2023.

[38] A. Guesmi, I. M. Bilasco, M. Shafique, and I. Alouani, "Advart: Adversarial art for camouflaged object detection attacks," *ArXiv*, vol. abs/2303.01734, 2023. [Online]. Available: https://api.semanticscholar.org/CorpusID:257353509

[39] R. Girshick, J. Donahue, T. Darrell, and J. Malik, "Rich feature hierarchies for accurate object detection and semantic segmentation," in *Proceedings of the IEEE Conference on Computer Vision and Pattern Recognition*, 2014, pp. 580–587.

[40] R. Girshick, "Fast r-cnn," in *Proceedings of the IEEE International Conference on Computer Vision*, 2015, pp. 1440–1448.

[41] X. Zhu, S. Lyu, X. Wang, and Q. Zhao, "Tph-yolov5: Improved yolov5 based on transformer prediction head for object detection on drone-captured scenarios," in *Proceedings of the IEEE/CVF International Conference on Computer Vision*, 2021, pp. 2778–2788.

[42] W. Ren, X. Wang, J. Tian, Y. Tang, and A. B. Chan, "Tracking-by-counting: Using network flows on crowd density maps for tracking multiple targets," *IEEE Transactions on Image Processing*, vol. 30, pp. 1439–1452, 2021.

[43] M. Huang, C. Hou, Q. Yang, and Z. Wang, "Reasoning and tuning: Graph attention network for occluded person re-identification," *IEEE Transactions on Image Processing*, vol. 32, pp. 1568–1582, 2023.

[44] Z. He, H. Zhao, J. Wang, and W. Feng, "Multi-level progressive learning for unsupervised vehicle re-identification," *IEEE Transactions on Vehicular Technology*, vol. 72, no. 4, pp. 4357–4371, 2023.

[45] Q. Zhang, R. Cong, C. Li, M.-M. Cheng, Y. Fang, X. Cao, Y. Zhao, and S. Kwong, "Dense attention fluid network for salient object detection in optical remote sensing images," *IEEE Transactions on Image Processing*, vol. 30, pp. 1305–1317, 2021.

[46] J. Wang, A. Liu, X. Bai, and X. Liu, "Universal adversarial patch attack for automatic checkout using perceptual and attentional bias," *IEEE Transactions on Image Processing*, vol. 31, pp. 598–611, 2021.

[47] Z. Wei, J. Chen, M. Goldblum, Z. Wu, T. Goldstein, Y.-G. Jiang, and L. S. Davis, "Towards transferable adversarial attacks on image and video transformers," *IEEE Transactions on Image Processing*, vol. 32, pp. 6346–6358, 2023.

[48] L. Huang, C. Gao, and N. Liu, "Erosion attack: Harnessing corruption to improve adversarial examples," *IEEE Transactions on Image Processing*, 2023.

[49] M. Lee and J. Z. Kolter, "On physical adversarial patches for object detection," in *ICML Workshop on Security and Privacy of Machine Learning*, Los Angeles, USA, Jun 2019.

[50] R. Duan, X. Ma, Y. Wang, J. Bailey, A. K. Qin, and Y. Yang, "Adversarial camouflage: Hiding physical-world attacks with natural styles," in *2020 IEEE/CVF Conference on Computer Vision and Pattern Recognition*, 2020, pp. 997–1005.

[51] I. J. Goodfellow, J. Pouget-Abadie, M. Mirza, B. Xu, D. Warde-Farley, S. Ozair, A. C. Courville, and Y. Bengio, "Generative adversarial nets," in *Conference on Neural Information Processing Systems*, 2014.

[52] B. G. Doan, M. Xue, S. Ma, E. Abbasnejad, and D. C. Ranasinghe, "Tnt attacks! universal naturalistic adversarial patches against deep neural network systems," *IEEE Transactions on Information Forensics and Security*, vol. 17, pp. 3816–3830, 2022.

[53] L. Huang, C. Gao, Y. Zhou, C. Xie, A. Yuille, C. Zou, and N. Liu, "Universal physical camouflage attacks on object detectors," *IEEE/CVF Conference on Computer Vision and Pattern Recognition*, pp. 717–726, 2020.

[54] X. Qi, K. Huang, A. Panda, M. Wang, and P. Mittal, "Visual adversarial examples jailbreak large language models," *arXiv preprint arXiv:2306.13213*, 2023.

[55] D. Lu, Z. Wang, T. Wang, W. Guan, H. Gao, and F. Zheng, "Set-level guidance attack: Boosting adversarial transferability of vision-language pre-training models," *ArXiv*, vol. abs/2307.14061, 2023. [Online]. Available: https://api.semanticscholar.org/CorpusID:260164714

[56] J. Zhang, Q. Yi, and J. Sang, "Towards adversarial attack on vision-language pre-training models," *Proceedings of the 30th ACM International Conference on Multimedia*, 2022. [Online]. Available: https://api.semanticscholar.org/CorpusID:249888984

[57] H. Ma, K. Xu, X. Jiang, Z. Zhao, and T. Sun, "Transferable black-box attack against face recognition with spatial mutable adversarial patch," *IEEE Transactions on Information Forensics and Security*, pp. 1–1, 2023.

[58] Z. Chen, B. Li, S. Wu, S. Ding, and W. Zhang, "Query-efficient decision-based black-box patch attack," *IEEE Transactions on Information Forensics and Security*, vol. 18, pp. 5522–5536, 2023.

[59] N. Dalal and B. Triggs, "Histograms of oriented gradients for human detection," in *2005 IEEE Computer Society Conference on Computer Vision and Pattern Recognition*, vol. 1, 2005, pp. 886–893 vol. 1.